Molecular Organization of Cholesterol in Polyunsaturated Membranes: Microdomain Formation

Michael R. Brzustowicz,*† Vadim Cherezov,‡ Martin Caffrey,‡ William Stillwell,†§ and Stephen R. Wassall*†

*Department of Physics, Indiana University Purdue University Indianapolis, Indianapolis, Indiana 46202-3273; †Medical Biophysics Program, Indiana University School of Medicine, Indianapolis, Indiana 46202-5122; ‡Biochemistry, Biophysics, and Chemistry, The Ohio State University, Columbus, Ohio 43210-1173; §Department of Biology, Indiana University Purdue University Indianapolis, Indianapolis, Indiana 46202-5132 USA

ABSTRACT   The molecular organization of cholesterol in phospholipid bilayers composed of 1,2-diarachidonylphosphatidylcholine (20:4–20:4PC), 1-stearoyl-2-arachidonylphosphatidylcholine (18:0–20:4PC), and 20:4–20:4PC/18:0–20:4PC (1/1 mol) was investigated by solid-state ^{2}H NMR and by low- and wide-angle x-ray diffraction (XRD). On the basis of distinct quadrupolar powder patterns arising from $[3\alpha\text{-}^2H_1]$cholesterol intercalated into the membrane and phase separated as solid, solubility $\chi_{chol}^{NMR} = 17 \pm 2$ mol% and tilt angle $\alpha_0 = 25 \pm 1°$ in 20:4–20:4PC were determined. The corresponding values in 18:0–20:4PC were $\chi_{chol}^{NMR} \geq 50$ mol% and $\alpha_0 = 16 \pm 1°$. Cholesterol solubility determined by XRD was $\chi_{chol}^{XRD} = 15 \pm 2$ mol% and $\chi_{chol}^{XRD} = 49 \pm 1$ mol% for 20:4–20:4PC and 18:0–20:4PC, respectively. XRD experiments show that the solid sterol is monohydrate crystals presumably residing outside the bilayer. The ^{2}H NMR spectrum for equimolar $[3\alpha\text{-}^2H_1]$cholesterol added to mixed 20:4–20:4PC/18:0–20:4PC (1/1 mol) membranes is consistent with segregation of cholesterol into 20:4–20:4PC and 18:0–20:4PC microdomains of <160 Å in size that preserve the molecular organization of sterol in the individual phospholipid constituents. Our results demonstrate unambiguously that cholesterol has low affinity to polyunsaturated fatty acids and support hypotheses of lateral phase separation of membrane constituents into sterol-poor/polyunsaturated fatty acid-rich and sterol-rich/saturated fatty acid-rich microdomains.

INTRODUCTION

Cholesterol modulates phospholipid organization within membranes (Finegold, 1993; McMullen and McElhaney, 1996). Its ordering of liquid crystalline membranes has long been recognized. In addition, cholesterol has been hypothesized to assist in the sorting of membrane phospholipids into highly organized complexes that provide a platform for specific protein function that has been described as rafts or microdomains (Rietveld and Simons, 1998). Differential miscibility among the diverse array of phospholipids that comprise membranes is thought to promote lateral phase separation into cholesterol-rich and cholesterol-poor regions. A recently proposed molecular mechanism implicates cholesterol's relative affinity for polyunsaturated versus saturated acyl chains (Mitchell and Litman, 1998; Huster et al., 1998; Brzustowicz et al., 1999; Polozova and Litman, 2000). Specifically, close proximity of the rigid steroid moiety to polyunsaturated acyl chains is prohibited by steric constraints imposed by motional restriction of multiple *cis* double bonds. Here, we use solid-state deuterium nuclear magnetic resonance (^{2}H NMR) and x-ray diffraction (XRD) to investigate the molecular organization of cholesterol in phospholipid membranes containing arachidonic acid ($20:4^{\Delta 5, 8, 11, 13}\ \omega$-6), which possesses a *cis* double bond at carbons 5, 8, 11, and 13. Our experiments

focus on cholesterol membrane solubility and molecular orientation, providing unequivocal evidence in favor of cholesterol's profoundly low affinity for highly unsaturated acyl chains.

The phase behavior of homoacid disaturated and heteroacid saturated-monounsaturated phosphatidylcholine (PC) membranes containing cholesterol has been examined extensively (Finegold, 1993). Incorporation of the sterol into the lamellar liquid crystalline (L_α) phase restricts acyl chain motion. Detailed phase diagrams for 1,2-dipalmitoylphosphatidylcholine (16:0–16:0PC), 1-palmitoyl-2-oleoylphosphatidylcholine (16:0–18:1$^{\Delta 9}$PC), and 1-palmitoyl-2-petroselinoylphosphatidylcholine (16:0–18:1$^{\Delta 6}$PC), constructed on the basis of solid-state NMR, identify a liquid-ordered (*lo*) state over a wide range of temperatures for membranes rich (>25 mol%) in cholesterol (Vist and Davis, 1990; Thewalt and Bloom, 1992; Huang et al., 1993). The properties of the lipid molecules in this phase resemble those of the familiar "fluid" L_α (also known as liquid disordered, or *ld*) phase, except that the acyl chains have restricted conformational freedom. Rapid axially symmetric reorientation of PC molecules about the bilayer normal, albeit slower than in the sterol-free bilayer, and a rate of lateral diffusion characteristic of the fluid phase are retained. At lower cholesterol content, the *lo* and *ld* phases coexist. The solubility limit is typically quoted at ≥50 mol% (Phillips, 1990), although as high as 66 mol% has been found for 16:0–16:0PC and 16:0–18:1PC[1] (Huang et al., 1999). Solid-state ^{2}H NMR of selectively deuterated

---

[1]The abbreviation 18:1 signifies the Δ9 isomer (oleic acid) hereon.

cholesterol has been used to directly observe membrane incorporated cholesterol (Oldfield et al., 1978; Bonmatin et al., 1990; Marsan et al., 1999; Brzustowicz et al., 1999). Similar molecular ordering and dynamics within homoacid disaturated and heteroacid saturated-monounsaturated PC membranes were indicated. The steroid moiety rotates rapidly in small, discrete steps around the long molecular axis, which fluctuates in orientation through a narrow range of angles slightly tilted relative to the bilayer normal. Hydrogen bonding between the 3β-hydroxyl of cholesterol and the carbonyls of phospholipids, possibly essential for proper alignment of the steroid moiety, has been debated (Guo and Hamilton, 1995).

Less is known about the interaction of cholesterol with polyunsaturated phospholipids. High levels of polyunsaturated fatty acid (PUFA), occasionally exceeding 50 mol%, are found in certain biomembranes (Salem et al., 1986). The nervous system accumulates phospholipids enriched in 20:4 and docosahexaenoic (22:6) acids. They are primarily esterified at the *sn*-2 position of the glycerol backbone whereas, as with the majority of phospholipids in vivo (Gennis, 1989), the *sn*-1 chain is usually saturated. Phospholipids with PUFA esterified to both *sn*-1 and *sn*-2 positions, however, are present in specialized membranes. In particular, they are abundant in retinal membranes (Aveldano, 1989). Nearly 30% of PCs isolated from bovine-rod outer segments, for example, are dipolyunsaturated. The relatively few studies published to date imply that the addition of cholesterol to heteroacid saturated-polyunsaturated and homoacid dipolyunsaturated PC membranes has the same general effect as seen in homoacid disaturated and heteroacid saturated-monounsaturated PCs (Mitchell and Litman, 1998; Brzustowicz et al., 1999; Jackman et al., 1999). Membranes become more ordered in the L_α state and the sterol reorients rapidly around a "wobbling" long molecular axis, irrespective of the presence of *sn*-2 polyunsaturation. Despite qualitative similarity in behavior, a major distinction exists between the molecular organization of cholesterol in homoacid dipolyunsaturated and heteroacid saturated-polyunsaturated PC bilayers. The solubility of cholesterol in 1,2-diarachidonylphosphatidylcholine (20:4–20:4PC) and 1,2-didocosahexaenoylphosphatidylcholine (22:6–22:6PC) is more than a factor of three times lower than in 1-stearoyl-2-arachidonylphosphatidylcholine (18:0–20:4PC) and 1-stearoyl-2-docosahexaenoylphosphatidylcholine (18:0–20:6PC), where an amount comparable with disaturated and saturated-monounsaturated PCs can be accommodated (Huster et al., 1998; Brzustowicz et al., 1999, 2000).

In a preliminary investigation, we were able to show that the solubility of cholesterol in 20:4–20:4PC bilayers is low (~15 mol%) because the ^{2}H NMR spectrum for a system with 50 mol% [3α-^{2}H$_1$]cholesterol revealed components corresponding to membrane-incorporated and phase-separated solid sterol (Brzustowicz et al., 1999). Two questions

inspired by this original finding are addressed in the current work. First, what is the form of the solid cholesterol (anhydrous or monohydrate crystals) phase separated from the membrane? Second, is cholesterol's differential miscibility and orientation between 20:4–20:4PC and 18:0–20:4PC conserved when cholesterol is added to a mixed-lipid 20:4–20:4PC/18:0–20:4PC system? We are motivated to answer the latter question by the possibility that introduction of sterol may cause the mixture to phase-separate, which would have the potential to drive the formation of microdomains or rafts in native cell membranes containing saturated (e.g., sphingomeylin) and highly unsaturated (e.g., dipolyunsaturated) lipids. Our study complements solid-state ^{2}H NMR with low- and wide-angle XRD. Solid-state ^{2}H NMR compares the molecular organization of equimolar [3α-^{2}H$_1$]cholesterol in three model membranes: 18:0–20:4PC, 20:4–20:4PC, and 20:4–20:4PC/18:0–20:4PC (1/1 mol). XRD corroborates the solubility measured by ^{2}H NMR and identifies the nature of the solid cholesterol in these systems.

MATERIALS AND METHODS

Materials

Avanti Polar Lipids (Alabaster, AL) was the source of 18:0–20:4PC and 20:4–20:4PC. Cholesterol deuterated at the 3α position, [3α-^{2}H$_1$]cholesterol, was obtained from Cambridge Isotope Laboratories, Inc. (Andover, MA) or was a gift from E. Oldfield (Oldfield et al., 1978). Cholesterol and butylated hydroxytoluene (BHT) were purchased from Sigma (St. Louis, MO), and deuterium-depleted water was purchased from Isotec Inc. (Miamisburg, OH). Lipids showed one spot by thin layer chromatography and were used without further purification.

Because of the sensitivity of polyunsaturated phospholipids to oxidation, all sample preparation occurred under a stream of nitrogen or in a nitrogen atmosphere within a home-built glovebox. Exposure to light was minimized. Water and buffer were thoroughly degassed. All samples were hydrated to 50 wt% H$_2$O. Specific details follow for each experimental approach. All experiments were performed at 20°C.

^{2}H NMR

Stock solutions of 50–100 mg phospholipid in chloroform were combined with dry [3α-^{2}H$_1$]cholesterol in appropriate ratios and the antioxidant BHT in degassed methanol was added (1:250 mol BHT relative to lipid). Initial drying of the organic solution under a nitrogen stream was followed by 12 h of vacuum pumping to remove residual solvent. The lipids were vortex-mixed at room temperature (~20°C) with 50 wt% 50 mM Tris buffer (pH 7.5) and the pH was adjusted to 7.5. Six lyophilizations with excess (1–2 ml) deuterium-depleted water were then performed to reduce naturally abundant ^{2}HHO. After final hydration with 50 wt% degassed deuterium-depleted water, the resultant samples consisting of an aqueous multilamellar dispersion were transferred to 5- or 7-mm NMR tubes and stored at −80°C. They were equilibrated at room temperature for 1 h before experimentation. All samples were verified to be in lamellar phase via the characteristic shape of their ^{1}H decoupled ^{31}P NMR spectra (Seelig, 1978).

^{2}H NMR powder pattern spectra were recorded on a home-built spectrometer operating at 27.6 MHz (McCabe and Wassall, 1997). Two probes, one home-built and the other constructed by Cryomagnet Systems, Inc.

(Indianapolis, IN), with 5- or 7-mm transverse mounted coils were used. The spectra were collected with a phase-alternated quadrupolar echo sequence ($90°_x − τ_2 − 90°_y − acquire − delay$)$_n$ (Davis et al., 1976). Unless stated otherwise, spectral parameters were: 90° pulse width = 2.1–4.2 μs; separation between pulses $τ_2$ = 75 μs; delay time between pulse sequences = 75 or 15 s; sweep width = ±500 kHz; dataset = 1K; and number of transients = 10,000–100,000. To increase signal-to-noise, experiments were conducted on resonance and the "out of phase" channel was zeroed before Fourier transformation. The consequent spectra are reflected around the central resonant frequency.

Additional ^{2}H NMR spectra were acquired at 76.7 MHz on another home-built spectrometer in the laboratory of R. J. Wittebort, University of Louisville (Zhang et al., 1998). Spectral parameters were comparable with those listed above.

Cholesterol orientation within membrane

The ^{2}H NMR spectrum from membrane incorporated [3α-^{2}H$_1$]cholesterol in an aqueous multilamellar dispersion is a superposition of doublets produced by random orientational distribution of lipid bilayers (Oldfield et al., 1978; Brzustowicz et al., 1999). The dominant peaks of the resultant powder pattern are characterized by residual quadrupolar splitting

$$\Delta v_r = \frac{3}{4}\left(\frac{e^2qQ}{h}\right)|S_{CD}|. \quad (1)$$

where e^2qQ/h (= 170 kHz) is the static quadrupolar coupling constant, and S_{CD} is an order parameter describing the angular fluctuations of the C-^{2}H bond with respect to the bilayer normal which constitutes the axis of motional averaging. Cholesterol's composite motion consists of rotation about its long molecular axis and libration of this axis with respect to the bilayer normal. The motions are axially symmetric and the order parameter may be written

$$S_{CD} = S_\gamma S_\alpha \quad (2)$$

where S_γ is a geometric factor

$$S_\gamma = \frac{1}{2}\left(3\cos^2\gamma - 1\right) \quad (3)$$

specified by the angle γ between the C-^{2}H bond and the molecular axis. Fig. 1 illustrates the disposition of angles and axes. Adopting a value for γ of 79° from previous work leads to $S_\gamma = -0.445$ (Taylor et al., 1981). The molecular order parameter S_α (often called S_{mol}) specifies cholesterol's libration in terms of a time average, denoted by angular brackets, of the angle α between the molecular axis and the bilayer normal (Fig. 1) (Petersen et al., 1977; Oldfield et al., 1978)

$$S_\alpha = \frac{1}{2}\langle 3\cos^2\alpha - 1\rangle \quad (4)$$

Assuming that an axially symmetric Gaussian distribution describes α, the most probable value α_0 (tilt angle) may be derived via numerical integration of

$$S_\alpha = \frac{\frac{1}{2}\int_0^\pi \sin(\alpha)\exp(-\alpha^2/2\alpha_0^2)(3\cos^2\alpha - 1)d\alpha}{\int_0^\pi \sin(\alpha)\exp(-\alpha^2/2\alpha_0^2)da}. \quad (5)$$
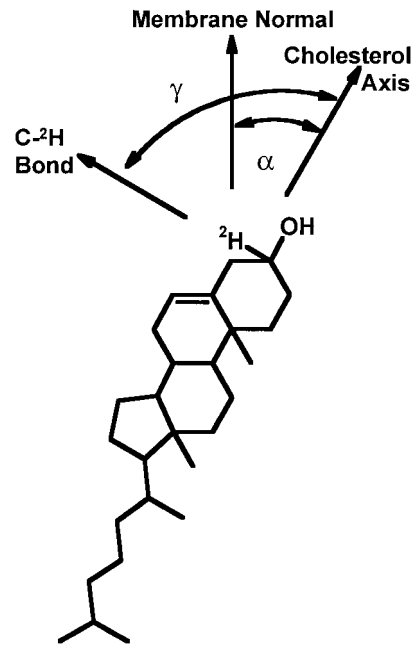

FIGURE 1 Angle and axis designation in membrane-intercalated [3α-^{2}H$_1$]cholesterol.

Membrane solubility of cholesterol

At concentrations above the solubility limit of cholesterol within a membrane, excess cholesterol is present as solid giving rise to a broad component ($\Delta v_Q \sim$ 118 kHz) in the ^{2}H NMR spectrum for [3α-^{2}H$_1$]cholesterol (Monck et al., 1993; Ruocco et al., 1996; Brzustowicz et al., 1999). Superimposed upon this signal is a distinct, much narrower ($\Delta v_r \sim$ 37–47 kHz) component attributable to membrane-intercalated cholesterol. The proportion of membrane-intercalated cholesterol corresponds directly to the fraction f_{int} of the total integrated intensity contributed by the narrow spectral component. This fraction may be determined via spectral simulation (Brzustowicz et al., 1999) or after depaking (Sternin et al. 1983; McCabe and Wassall, 1997). The latter approach deconvolutes a spectrum of single alignment from the powder signal, thereby resolving an individual doublet for each component. Membrane solubility of cholesterol is then calculated with

$$\chi_{chol}^{NMR} = \frac{f_{int}}{f_{PC} + f_{int}} \quad (6)$$

where f_{PC} is the molar fraction of phospholipid relative to total cholesterol.

Accounting for differences in relaxation rate between cholesterol inside and outside the membrane is crucial to an accurate determination of χ_{chol}^{NMR} (Brzustowicz et al., 1999). The spin lattice relaxation time for [3α-^{2}H$_1$]cholesterol intercalated in membranes is $T_{1Z} \sim$3ms, whereas the corresponding value for solid [3α-^{2}H$_1$]cholesterol is $T_{1Z} \sim$3s (Brzustowicz and Wassall, unpublished results). The delay between pulse sequences must be sufficiently long, (5T_{1Z} = 15 s) to ensure observation of full intensity signals from both spectral components. In contrast, their spin-spin relaxation times ($T_{2e} \sim$200 μs) are nearly equivalent (Brzustowicz and Wassall, unpublished results), and correction is unnecessary to compensate for differential relaxation during the time, $2\tau_2$, before echo formation in the pulse sequence.

XRD

Stock solutions of cholesterol and phospholipid in chloroform were codissolved in appropriate ratios with total lipid mass between 5 and 10 mg. The samples were dried with a stream of nitrogen gas and subsequent vacuum pumping in the dark for 6 h. They were then vortex-mixed with 50 wt% 50-mM Tris buffer (pH 7.5) at room temperature until they appeared homogenous by visual inspection. The resultant aqueous multilamellar dispersions were transferred to 1 mm outside diameter quartz capillary tubes (Charles Supper Co., Natick, MA) and centrifuged for ~5 min to pellet the sample at the sealed end of the capillary tubes. After centrifugation, the capillary tubes were flame-sealed and a bead of quick-drying epoxy was applied to ensure the integrity of the flame seal. Samples were stored in dry ice and incubated at 20°C for at least 1 h before experiments.

Another procedure for sample preparation, low temperature trapping (LTT), was also used (Huang et al., 1999). The initial removal of organic solvent with a gentle stream of nitrogen gas was followed by addition of 100 μl dry chloroform containing 1% (by volume) methanol. The samples were frozen in liquid nitrogen and vacuum pumped for 6 h at 50 mTorr. The samples were kept cold with dry ice during this period. Residual solvent was removed under vacuum at −20°C for another ~12 h. The resultant powders were placed in a stirring, room temperature water bath for 1 min and brought to room temperature. They were immediately hydrated with 50 wt% 50 mM Tris buffer (pH 7.5) and vortex-mixed for 1 min.

XRD measurements were performed using a rotating anode x-ray generator (Rigaku RU-300 working at 45 kV and 250 mA) producing Ni filtered Cu K$_\alpha$ radiation (wavelength λ = 1.5418 Å). Two curved Ni-coated mirrors (Charles Supper Co.) focus the x-ray beam to a spot size of ~1 × 0.5 mm^2 (horizontal × vertical) at the detector position. Sample-to-detector distance, typically 250 mm, was measured using a silver behenate standard (Blanton et al., 1995). Samples were placed in a home-built sample-holder with space for seven samples (Zhu and Caffrey, 1993). The sample was continuously translated at a rate of 3 mm/min back and forth along a 6-mm section of the sample to average the contributions to total scattering from different parts of the sample and to minimize possible radiation damage effects during long exposures. The temperature inside the sample holder was regulated by two thermoelectric Peltier effect elements controlled by a computer feedback system. Measurements were performed at T = 20.0 ± 0.05°C. Typical exposure time was 2 h. High-resolution image plates measuring 250 × 200 mm^2 (HR-IIIn, Fuji Medical Systems, Stamford, CT) were used to record diffraction patterns. X-ray images from the image plates were obtained after exposure using a phosphorimage scanner (Storm-840, Molecular Dynamics, Sunnyvale, CA) with 100-μm resolution. The large size of the image plates allows simultaneous registration of low- and wide-angle diffraction patterns spanning reciprocal vector space, q (= $4\pi \sin \theta/\lambda$), from 0.05 to 1.84 Å^{-1} (corresponding, respectively, to a real space range of 125 Å to 3.4 Å). Intensity versus scattering vector plots (I-q) were obtained by radial integration of static two-dimensional (2-D) diffraction patterns using the program FIT2D (Hammersley, 1997). Peaks in the I-q plots were fitted with Peakfit 4.0 (SPSS Inc., Chicago, IL) to locate peak positions and determine integrated intensities.

Form of membrane-excluded cholesterol

The presence of cholesterol crystals that have phase separated from the bilayer in multilamellar vesicles is evidenced by a unique set of sharp diffraction powder rings in addition to the lamellar reflections from lipid multilamellar vesicles. The diffraction patterns for both anhydrous and monohydrate cholesterol are known and were used for purposes of identification (Craven, 1976; Shieh et al., 1977; Loomis et al., 1979). To avoid ambiguity because of overlap of the first order of cholesterol diffraction with lamellar diffraction peaks from the bilayers, only the 002, 020, and 200 cholesterol peaks were used. For cholesterol monohydrate, the respec-

tive reciprocal and real spacings are (002) 0.3701 Å^{-1}, 17.0 Å; (020) 1.033 Å^{-1}, 6.079 Å; and (200) 1.044 Å^{-1}, 6.015 Å. For anhydrous cholesterol, the respective reciprocal and real spacings are (002) 0.3709 Å^{-1}, 16.9 Å; (020) 0.8924 Å^{-1}, 7.037 Å; and (200) 1.203 Å^{-1}, 5.22 Å.

Membrane solubility of cholesterol

Samples were prepared with concentrations of cholesterol around the solubility limit determined by ^{2}H NMR. For samples where cholesterol crystals were present, the combined integrated intensities of the 002, 020, and 200 reflections (normalized with respect to the integrated intensity of the lipid wide-angle peak) were plotted against mol% cholesterol. Linear extrapolation of these plots to zero intensity gives the cholesterol solubility limit $\chi_{\text{chol}}^{\text{XRD}}$, with an accuracy of ~±1 mol%.

RESULTS

^{2}H NMR

Aqueous multilamellar dispersions of 20:4–20:4PC/[3α-^{2}H$_1$]cholesterol (1/1 mol), 18:0–20:4PC/[3α-^{2}H$_1$]cholesterol (1/1 mol), and 20:4–20:4PC/18:0–20:4PC/[3α-^{2}H$_1$]cholesterol (1/1/2 mol) were prepared in 50 wt% Tris (pH 7.5). ^{2}H NMR spectra recorded at 20°C for the three systems are shown in Fig. 2.

Fig. 2 *A* is the spectrum for 20:4–20:4PC/[3α-^{2}H$_1$]cholesterol (1/1 mol). As can be clearly seen, it is a superposition of a relatively narrow powder pattern upon a broad pattern establishing that [3α-^{2}H$_1$]cholesterol exists in two motionally distinct pools. Quadrupolar splittings $\Delta \nu_r$ = 33 ± 1 kHz and $\Delta \nu_Q$ = 118 ± 1 kHz, respectively, characterize the two powder patterns. The broad spectral component ($\Delta \nu_Q$ = 118 ± 1 kHz) corresponds to solid [3α-^{2}H$_1$]cholesterol, which is presumably located outside the bilayer (Monck et al., 1993; Ruocco et al., 1996; Brzustowicz et al., 1999). Membrane-intercalated [3α-^{2}H$_1$]cholesterol is responsible for the narrow component (Oldfield et al., 1978; Brzustowicz et al., 1999). Axially symmetric, rapid reorientation about the bilayer normal reduces the splitting to the residual value measured ($\Delta \nu_r$ = 33 ± 1 kHz) from which an order parameter S_{CD} (= 0.26) for the 3α C-^{2}H bond may be calculated with Eq. 1. The molecular order parameter determined from S_{CD} via Eq. 2 is S_α = 0.58. On the assumption that a weighted Gaussian distribution applies to orientation of the wobbling steroid moiety, S_α can then be matched with numerically integrated values (Eq. 5) to extract a most probable (tilt) angle α_0 relative to the bilayer normal (Petersen et al., 1977; Oldfield et al., 1978). The tilt angle derived in this manner for [3α-^{2}H$_1$]cholesterol incorporated into 20:4–20:4PC bilayers is α_0 = 25 ± 1°.

The signal from solid [3α-^{2}H$_1$]cholesterol in Fig. 2 *A* indicates that less than an equimolar amount of sterol incorporates into dipolyunsaturated 20:4–20:4PC membranes. An estimate of the solubility limit may be obtained on the basis of relative integrated intensity of the spectral components ascribed to membrane-intercalated and solid
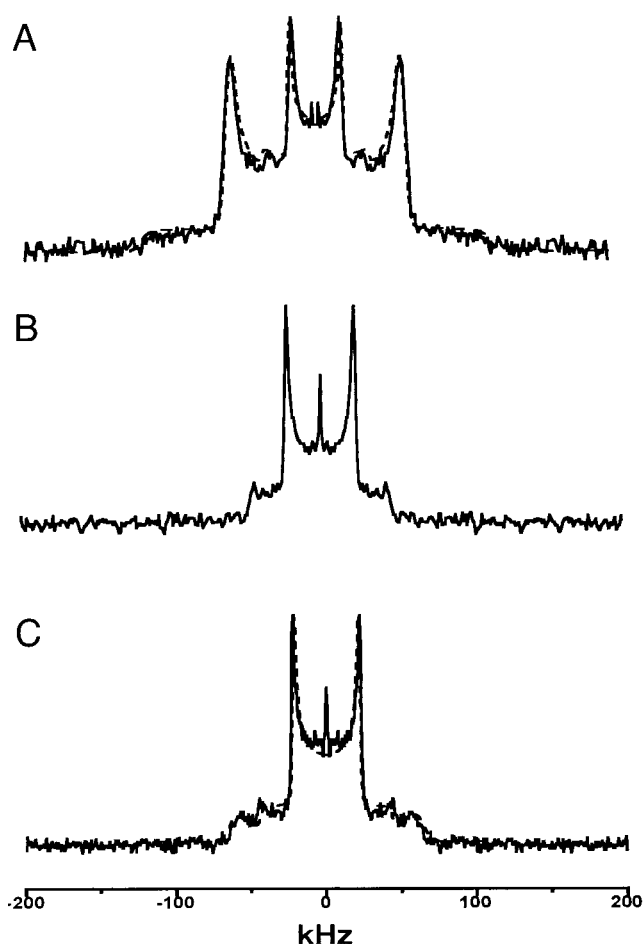
FIGURE 2 ^{2}H NMR spectra at 20°C for 50 wt% aqueous multilamellar dispersions in 50 mM Tris (pH 7.5) of (*A*) 20:4–20:4PC/[3α-^{2}H$_1$]cholesterol (1/1 mol), (*B*) 18:0–20:4PC/[3α-^{2}H$_1$]cholesterol (1/1 mol), and (*C*) 20:4–20:4PC/18:0–20:4PC/[3α-^{2}H$_1$]cholesterol (1/1/2 mol). The dashed lines in (*A*) and (*C*) are simulations composed of a narrow powder pattern assigned to [3α-^{2}H$_1$]cholesterol intercalated into the membrane superposed upon a broad powder pattern from solid [3α-^{2}H$_1$]cholesterol. Spectral parameters were as described in Materials and Methods. Line broadening was applied as follows: (*A*) Gaussian multiplication (GM) = 2.5 kHz, (*B*) and (*C*) GM = 1 kHz.

[3α-^{2}H$_1$]cholesterol (Brzustowicz et al., 1999). The dashed line superposed upon the experimental data represents a simulation comprised of the respective components in a 20:80 ratio of intensity which translates into $f_{int} = 0.20$ for the intercalated fraction. Substitution into Eq. 6, recognizing $f_{PC} = 1.00$ as the fraction of phospholipid with respect to total cholesterol, yields $\chi_{chol}^{NMR} = 17$ mol% for the solubility. The uncertainty is assessed to be ±2 mol%.

In Fig. 2 *B*, the ^{2}H NMR spectrum for 18:0–20:4PC/[3α-^{2}H$_1$]cholesterol (1/1 mol) is displayed as a control. It contains only one powder pattern with residual splitting $\Delta\nu_r = 45 \pm 1$ kHz which is assigned to sterol within the membrane. The corresponding molecular order parameter and tilt angle are $S_\alpha = 0.79$ and $\alpha_o = 16 \pm 1°$. A broad component

denoting the presence of solid [3α-^{2}H$_1$]cholesterol ($\Delta\nu_Q \sim$ 118 kHz) is not visible. Under the experimental conditions used, in particular the delay of 15 s between repetition of the quadrupolar sequence (Brzustowicz et al., 1999), such a signal would be detected if solid cholesterol were present. The absence of a broad spectral component in Fig. 2 *B* demonstrates that all the [3α-^{2}H$_1$]cholesterol added to 18:0–20:4PC incorporates into the membrane. From this observation, a solubility of $\chi_{chol}^{NMR} \geq 50$ mol% may be inferred. The significant increase in tilt angle and drastic reduction in membrane solubility identified from our interpretation of the spectra for [3α-^{2}H$_1$]cholesterol in 20:4–20:4PC (Fig. 2 *A*) compared with 18:0–20:4PC (Fig. 2 *B*) demonstrate markedly different molecular organization of cholesterol in the bilayer of homoacid dipolyunsaturated versus heteroacid saturated-polyunsatuarated phospholipid.

To test whether the differences in behavior seen here for cholesterol in single-component membranes would be manifest in a system more akin to a natural membrane of heterogeneous composition, the mixed 18:0–20:4PC/20:4–20:4PC/[3α-^{2}H$_1$]cholesterol (1/1/2 mol) system was examined by ^{2}H NMR. In the ensuing spectrum shown in Fig. 2 *C*, there are two spectral components assigned to membrane-intercalated ($\Delta\nu_r = 44 \pm 1$ kHz) and solid ($\Delta\nu_Q = 118 \pm 1$ kHz) [3α-^{2}H$_1$]cholesterol. A molecular order parameter of $S_\alpha = 0.77$ is calculated from the splitting of the former signal and equates to tilt angle $\alpha_0 = 17 \pm 1°$. The dashed line superimposed upon the experimental data is a simulation with signals attributable to membrane-intercalated and solid [3α-^{2}H$_1$]cholesterol in a 68:32 ratio of integrated intensity, which gives $\chi_{chol}^{NMR} = 40 \pm 2$ mol% for the solubility of the sterol in the mixed 18:0–20:4PC/20:4–20:4PC system. The observation of only a single signal from sterol incorporated into the mixed membrane is significant. It implies that, in the possibilty that separate, distinct 20:4–20:4PC/[3α-^{2}H$_1$]cholesterol and 18:0–20:4/[3α-^{2}H$_1$]cholesterol domains were to exist, exchange between them must occur more quickly than the timescale of 2×10^{-5} s to which the ^{2}H NMR experiment is sensitive (Bloom and Thewalt, 1995). This issue will be elaborated later in the Discussion.

Spectral parameters derived from a simulation are not necessarily unique. Specifically, the estimates of solubility χ_{chol}^{NMR} obtained from the spectra in Fig. 2 suffer from their dependence upon the parameters input for line broadening. These parameters are indeterminate, and a range of them will provide a "best fit" to the experimental data. Depaking is an approach that avoids this, albeit somewhat minor, drawback (Sternin et al. 1983; McCabe and Wassall, 1997). The procedure numerically deconvolutes powder pattern spectra governed by axially symmetric, second rank tensor interactions to spectra characteristic of a sample of single alignment oriented with the axis of symmetry parallel to the magnetic field. The resultant depaked spectra in the case of ^{2}H NMR contain doublets split by twice the frequency of the peaks in the powder pattern and whose intensity may be
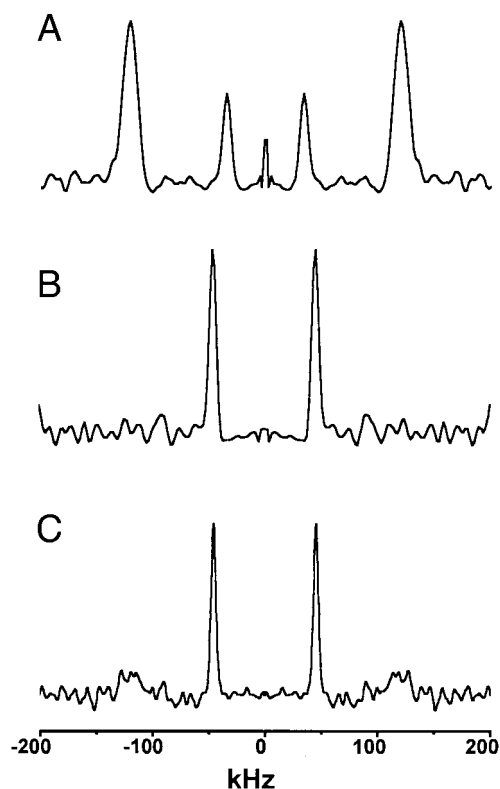
FIGURE 3   Depaked ^{2}H NMR spectra at 20°C for 50 wt% aqueous multilamellar dispersions in 50 mM Tris (pH 7.5) of (*A*) 20:4–20:4PC/[3α-^{2}H$_1$]cholesterol (1/1 mol), (*B*) 18:0–20:4PC/[3α-^{2}H$_1$]cholesterol (1/1 mol), and (*C*) 20:4–20:4PC/18:0–20:4PC/[3α-^{2}H$_1$]cholesterol (1/1/2 mol). They were iteratively depaked from the corresponding spectra in Fig. 2. Six iterations of the depaking program were performed.

then evaluated by straightforward numerical integration without simulation.

The depaked counterparts of the spectra in Fig. 2 are plotted in Fig. 3. They illustrate the enhancement in resolution achieved. The two superposed narrow and broad powder patterns observed in Fig. 2 *A* for 20:4–20:4PC/[3α-^{2}H$_1$]cholesterol (1/1 mol) become a pair of well resolved inner and outer doublets in Fig. 3 *A*. The doublets are split by 68 ± 2 kHz and 240 ± 2 kHz from, respectively, membrane-intercalated and solid sterol. Integrating each signal yields a ratio of 21:79 for their relative intensity. This ratio equates to a solubility of $\chi_{chol}^{NMR} = 17 \pm 2$ mol% for [3α-^{2}H$_1$]cholesterol in homoacid dipolyunsaturated 20:4–20:4PC. Fig. 3 *B* confirms that the situation contrasts in heteroacid saturated-polyunsaturated 18:0–20:4PC. Consistent with the single powder pattern seen for 18:0–20:4PC/[3α-^{2}H$_1$]cholesterol (1/1 mol) in Fig. 2 *B*, in Fig. 3 *B* only one doublet split by 92 ± 2 kHz because of membrane-intercalated [3α-^{2}H$_1$]cholesterol is discernible after depaking. There is no outer doublet with splitting ~240 kHz from solid [3α-^{2}H$_1$]cholesterol, which corroborates that the solubility in 18:0–20:4PC is $\chi_{chol}^{NMR} \geq 50$ mol%. Two doublets

with splittings 90 ± 2 kHz and 240 ± 2 kHz attributable to membrane-intercalated and, as expected, solid sterol are apparent in the depaked spectrum presented in Fig. 3 *C* for 20:4–20:4PC/18:0–20:4/[3α-^{2}H$_1$]cholesterol (1/1/2 mol). The respective integrated intensities are in the ratio 69:31 and correspond to solubility $\chi_{chol}^{NMR} = 41 \pm 2$ mol% in the mixture of phospholipids. Reassuringly, in each case the solubilities determined after depaking confirm within experimental uncertainty the estimates obtained by simulation of powder patterns.

XRD

Low- and wide-angle XRD patterns were collected at 20°C as a function of the concentration of cholesterol added to 20:4–20:4PC, 18:0–20:4PC and 20:4–20:4PC/18:0–20:4PC (1/1 mol) bilayers hydrated to 50 wt% in Tris buffer (pH 7.5). Integrated radial intensity profiles plotted against reciprocal space, I-q plots, are shown in Fig. 4. They are cropped from $q = 0.25$ to 2.0 Å^{-1}, focusing upon the region where the second-order peaks from cholesterol monohydrate or anhydrous cholesterol occur when solid sterol is present (Craven, 1976; Shieh et al., 1977; Loomis et al., 1979). A representative example of a complete spectrum is also included in the figure (Fig. 4 *D*). The broad peak centered at ~1.38 Å^{-1} (4.6 Å) is the lipid wide-angle peak resulting from lateral correlations between lipid chains. Its total area is proportional to the number of molecules in the bilayer and serves as a scaling factor for the area of other peaks within a diffraction pattern.

Fig. 4 *A* shows the results from 20:4–20:4PC/cholesterol in which the mol fraction of sterol is varied from $\chi_{chol} = 10$ to 30 mol% in 5 mol% increments. Crystalline cholesterol produces the labeled peaks (Craven, 1976; Shieh et al., 1977; Loomis et al., 1979). They emerge when $\chi_{chol} = 15$ mol% and grow in intensity as χ_{chol} increases, but are absent for $\chi_{chol} = 10$ mol%. Although the peak at 0.37 Å^{-1} ($d = 17.0$ Å) may correspond to the 002 reflection of either cholesterol monohydrate or anhydrous cholesterol; only the 020 and 200 reflections for cholesterol monohydrate were observed at respective positions 1.03 Å^{-1} ($d = 6.08$ Å) and 1.04 Å^{-1} ($d = 6.02$ Å). Peaks at 0.8924 Å^{-1} ($d = 7.037$ Å) and 1.203 Å^{-1} ($d = 5.22$ Å) for the equivalent reflections of anhydrous cholesterol were not observed. The data unambiguously identify the crystalline cholesterol to be in monohydrate form.

The normalized, summed integrated intensities of the three second-order reflections from cholesterol monohydrate in Fig. 4 *A* are plotted against cholesterol concentration in Fig. 5. A linear extrapolation to zero intensity intercepts at $\chi_{chol} = 15 \pm 2$ mol%. The intercept represents the solubility of cholesterol (χ_{chol}^{XRD}) in 20:4–20:4PC. Smaller amounts of sterol entirely intercalate into the bilayer. Solid cholesterol and the resultant diffraction peaks are only present at higher content exceeding the solubility limit. The
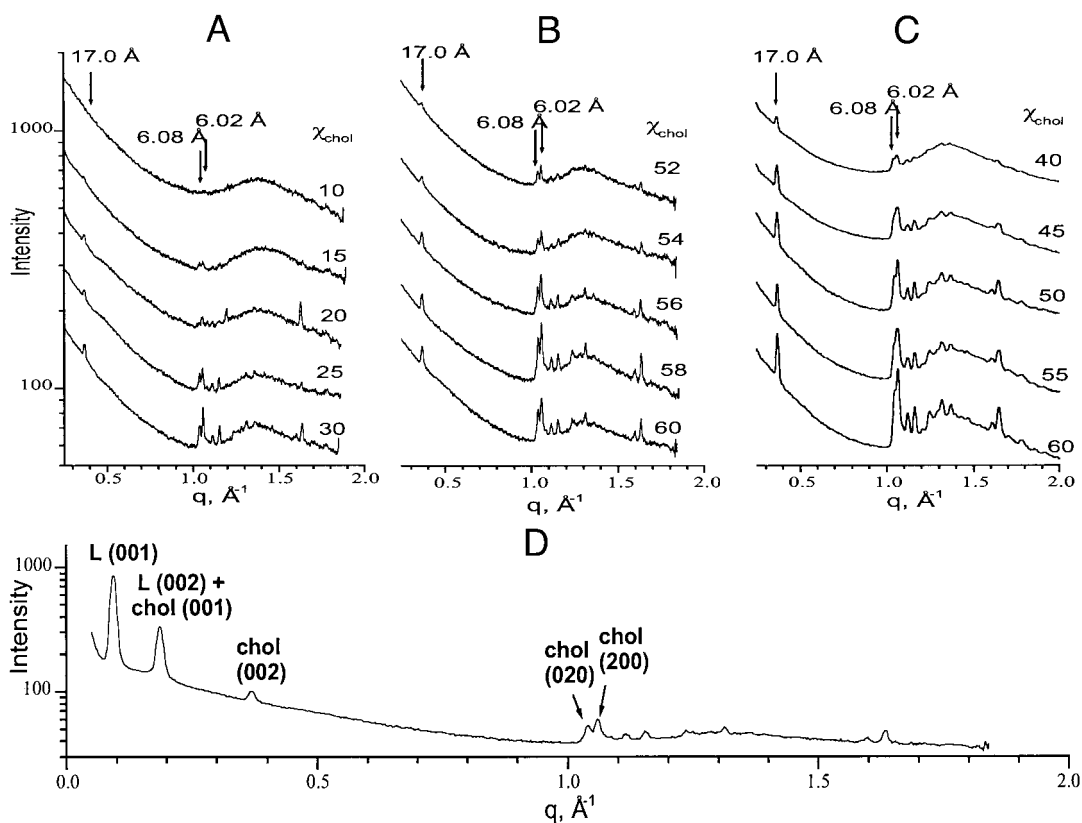
FIGURE 4 Integrated XRD radial intensity profiles at 20°C for 50 wt% aqueous multilamellar dispersions in 50 mM Tris (pH 7.5) of (A) 20:4–20:4PC/cholesterol, (B) 18:0–20:4PC/cholesterol, and (C) 20:4–20:4PC/18:0–20:4PC(1/1 mol)/cholesterol. Concentration of cholesterol χ_{chol} is indicated in mol%. Plots A–C are cropped from $q = 0.25$ Å^{-1} to $q = 2.00$ Å^{-1} in reciprocal space to focus upon the 002 (17.0 Å), 020 (6.08 Å), and 200 (6.02 Å) diffraction peaks (arrows) from cholesterol monohydrate used for quantitation in Fig. 5. The entire spectrum for a sample containing 18:0–20:4PC/cholesterol ($\chi_{chol} = 60$ mol%) is presented in (D) which shows the first two reflections from lipid multilayers. The 002 reflection from the latter and the 001 reflection from the cholesterol crystal overlap. The intensity scale is arbitrary and, to aid observation of small peaks, logarithmic. Individual curves are shifted evenly along the intensity axis.

failure to detect diffraction peaks from solid cholesterol in 20:4–20:4PC when $\chi_{chol} = 11$, 12, 13, or 14 mol% (data not shown) lends further support to the reliability of our estimate of 15 ± 2 mol% for χ_{chol}^{XRD}.

XRD patterns for 18:0–20:4PC/cholesterol where χ_{chol} varies from 52 to 60 mol% in 2-mol% increments are displayed in Fig. 4 B. Reflections from cholesterol monohydrate which are barely discernible at the lowest concentration of $\chi_{chol} = 52$ mol% and then increase in intensity with concentration of cholesterol are visible in all samples. As with 20:4–20:4PC, no peaks from anhydrous cholesterol were detected. A graph of the normalized sum of the integrated intensities of the three second-order repeats from cholesterol monohydrate versus cholesterol concentration is drawn in Fig. 5. The solubility of sterol in 18:0–20:4PC deduced by linear extrapolation of the data to zero intensity is $\chi_{chol}^{XRD} = 49 \pm 1$ mol%.

The diffraction profiles in Fig. 4 C are for 20:4–20:4PC/18:0–20:4PC(1/1mol)/cholesterol samples in which χ_{chol} varies from 40 to 60 mol% in 5-mol% increments. Reflec-

tions for cholesterol monohydrate that become greater in intensity with increased content of the sterol are clearly present in each profile, whereas peaks from anhydrous cholesterol were again not found. A solubility limit of $\chi_{chol}^{XRD} = 36 \pm 3$ mol% in 20:4–20:4PC/18:0–20:4PC (1/1 mol) is estimated on the basis of linear extrapolation to zero intensity in a plot against cholesterol concentration of the normalized, summed integrated intensities of the three second-order repeats from cholesterol monohydrate (Fig. 5).

DISCUSSION

Dipolyunsaturated phospholipid membranes

Cholesterol solubility

The results obtained in this study are summarized in Table 1. They establish unquestionably that the molecular organization of cholesterol within dipolyunsaturated PC bilayers differs radically from within disaturated or mixed acyl saturated-polyunsaturated PC bilayers. The reduction in mem-
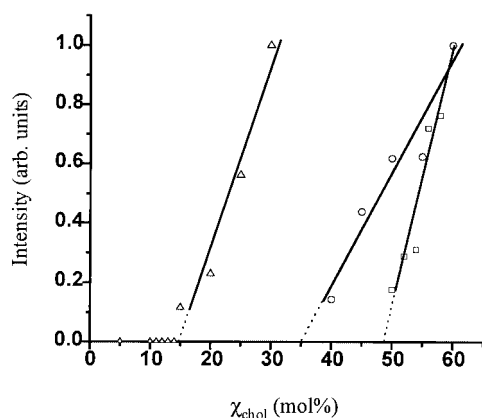
FIGURE 5 Combined integrated intensity of second-order XRD peaks (002, 020, and 200) from cholesterol monohydrate versus concentration of cholesterol at 20°C for 50 wt% aqueous multilamellar dispersions in 50 mM Tris (pH 7.5) of △ 20:4–20:4PC/cholesterol, □ 18:0–20:4PC/cholesterol, and ○ 20:4–20:4PC/18:0–20:4PC(1/1 mol)/cholesterol.

brane solubility seen in fully hydrated bilayers of 20:4–20:4PC represents the most dramatic manifestation. By solid-state ^{2}H NMR and XRD solubility limits of $\chi_{\rm chol}^{\rm NMR} = 17 \pm 2$ mol% and $\chi_{\rm chol}^{\rm XRD} = 15 \pm 1$ mol%, respectively, were measured. The agreement of the estimates is within experimental uncertainty and demonstrates the efficacy of these complementary techniques which both rely upon the detection of solid cholesterol. In the former case solubility is calculated from the relative integrated intensity of distinct spectral components attributable to membrane-intercalated and solid [3α-^{2}H$_1$]cholesterol (Figs. 2 and 3), whereas the concentration when XRD peaks from solid sterol begin to appear defines the solubility limit in the latter case (Figs. 4 and 5). A slight overestimation by NMR is to be expected as distortion effects associated with the finite width of excitation pulses in the quadrupolar sequence increasingly attenuate spectral features farther from the resonant frequency (Bloom et al., 1980). The presence of diffraction peaks at $q = 1.03$ Å^{-1} (020) and 1.04 Å^{-1} (200) in Fig. 4 identify the solid cholesterol to be monohydrate crystals (Craven, 1976; Shieh et al., 1977; Loomis et al., 1979), which is the

form that was recognized for cholesterol exceeding the solubility limit in earlier work on less unsaturated model membrane systems (Guo and Hamilton, 1995; Sömjen et al., 1995; Huang et al., 1999). Diffraction peaks at $q = 0.89$ Å^{-1} (020) and 1.20 Å^{-1} (200), characteristic of the alternative anhydrous form in which solid cholesterol can exist, were absent. We were unable to make this designation on the basis of ^{2}H NMR in our preliminary report on 20:4–20:4PC because spectra for anhydrous and monohydrate [3α-^{2}H$_1$]cholesterol are indistinguishable (Brzustowicz et al., 1999).

The situation in 20:4–20:4PC membranes differs markedly from the solubility of ~50 mol% indicated for cholesterol in 18:0–20:4PC membranes by ^{2}H NMR (Figs. 2 B and 3 B) and XRD (Figs. 4 B and 5). The much higher value in the heteroacid saturated-polyunsaturated PC is consistent with solubilities usually found in phospholipid membranes (Phillips, 1990; Huang et al., 1999). In contrast, the low solubility of sterol seen in 20:4–20:4PC seems to be associated with dipolyunsaturation. Solid-state ^{2}H NMR and XRD data revealing ~10 mol% solubility in 22:6–22:6PC membranes (Brzustowicz et al., 2000) support this assertion. The formation of a separate crystalline phase, moreover, was implied by the failure of ^{1}H magic-angle spinning (MAS) NMR experiments to detect most of the signals from equimolar cholesterol added to 22:6–22:6PC membranes (Huster et al., 1998).

The possibility that artifactual crystallization of cholesterol occurred during preparation of our samples was considered. A variable reduction in solubility was seen by Huang et al. (1999) because of demixing of cholesterol from phospholipid when the sample was passed through an intermediate dry-state. Such a step, as in the protocol used in this work, is unavoidable. To overcome the problem, they developed a LTT method to trap the lipids in a well mixed state by lyophilizing at low temperature (−20°C). To test the validity of our results, we also performed XRD experiments on 20:4–20:4PC/cholesterol and 18:0–20:4PC/cholesterol samples prepared using the LTT approach. The solubilities measured (data not shown) agreed within experimental uncertainty with those determined on our conventionally prepared samples. We conclude that the much lower solubility observed for cholesterol in 20:4–20:4PC than in 18:0–20:4PC is not an artifact of sample preparation method. A fundamentally different interaction between cholesterol and polyunsaturated acyl chains as compared with saturated or monounsaturated acyl chains is responsible.

The existence of patches of cholesterol monohydrate as a bilayer within the plane of human ocular lens-fiber plasma membranes was recently hypothesized in a study of corneal lipid extracts containing cholesterol and phospholipid in concentrations corresponding to 71 and 77 mol% sterol (Jacob et al., 1999). The hypothesis was based upon interpretation of small-angle XRD patterns in terms of an immiscible cholesterol domain with unit cell periodicity of

TABLE 1 Compilation of data on the molecular organization of cholesterol added to 20:4–20:4PC, 18:0-20:4PC and 20:4-20:4/18:0-20:4PC (1/1 mol) membranes

	20:4-20:4PC	18:0-20:4PC	20:4-20:4PC/ 18:0-20:4PC (1/1 mol)
$\Delta\nu_r$ (kHZ)	33	45	44
S_{CD}	0.26	0.35	0.35
S_α	0.58	0.79	0.77
α_0	25°	16°	17°
$\chi_{\rm chol}^{\rm NMR}$ (mol%)	17	≥50	40
$\chi_{\rm chol}^{\rm XRD}$ (mol%)	15	49	36

Experimental conditions and uncertainties are as stated in the text.

34.0 Å. Such a 2-D arrangement is inapplicable to the solid cholesterol identified with 20:4–20:4PC membranes because the 002, 020, and 200 peaks from cholesterol monohydrate seen in our wide-angle XRD patterns (Fig. 4) signify 3-D crystals. In addition, it has been argued that exposure to water would render a pure cholesterol bilayer domain energetically unfavorable and cause subsequent crystallization out of the membrane (Huang and Feigenson, 1999). We conclude that the solid sterol detected here by ^{2}H NMR and XRD was excluded from the membrane. Observation of cholesterol monohydrate crystals in our samples by polarized optical microscopy substantiate this assessment (Brzustowicz and Williams, unpublished results).

Cholesterol orientation

Analysis of the quadrupolar splittings for the spectral component ascribed to $[3\alpha\text{-}^2H_1]$cholesterol intercalated into 20:4–20:4PC membranes, $\Delta\nu_r = 33 \pm 1$ kHz (Fig. 2 *A*), and 18:0–20:4PC membranes, $\Delta\nu_r = 45 \pm 1$ kHz (Fig. 2 *B*), provides further indication of a substantial distinction in molecular interaction. On the 10^{-6} s timescale sensed by ^{2}H NMR spectra, rapid reorientation about the long molecular axis and wobbling relative to the bilayer normal of $[3\alpha\text{-}^2H_1]$cholesterol reduce the static quadrupolar splitting to a residual value characteristic of the order parameter S_{CD} of the 3α C-^{2}H bond (Eq. 1) (Oldfield et al., 1978; Brzustowicz et al., 1999). Geometrical arguments (Eq. 2) relate S_{CD} to the molecular order parameter S_α defined in Eq. 4 which describes the fluctuations in orientation of the steroid moiety (Taylor et al., 1981). Interpretation then necessitates a model be invoked to specify the distribution $g(\alpha)$ of angles α the molecular axis makes with the bilayer normal. Following the precedent of earlier work, we applied a $\sin\alpha$ population weighted Gaussian function $g(\alpha) = \exp[-\alpha^2/2\alpha_0]$ to evaluate the most probable angle α_0 from S_α via Eq. 6 (Oldfield et al., 1978; Brzustowicz et al., 1999).

Table 1 compiles the tilt-angle data. Accordingly, the respective values $\alpha_0 = 25 \pm 1°$ vs. $\alpha_0 = 16 \pm 1°$ were deduced for $[3\alpha\text{-}^2H_1]$cholesterol within 20:4–20:4PC and 18:0–20:4PC membranes. The smaller angle of most probable tilt in 18:0–20:4PC is typical of the orientation found for the sterol in fully hydrated bilayers comprised of homoacid disaturated PCs and heteroacid saturated-unsaturated PCs. Tilt angles derived from previously published ^{2}H NMR data over a wide range of temperatures (10–60°C) and concentrations of sterol (10–50 mol%) fall within a narrow range $\alpha_0 = 15–20°$ irrespective of the degree of unsaturation in the *sn*-2 chain (Oldfield et al., 1978; Taylor et al., 1981, 1982; Murari et al., 1986; Brzustowicz et al., 1999). For instance, the value of $\alpha_0 = 16°$ measured here in 18:0–20:4PC is identical to that found for equimolar $[3\alpha\text{-}^2H_1]$cholesterol in 16:0–16:0PC, 18:0–18:1PC, and 18:0–22:6PC bilayers (Murari et al., 1986; Brzustowicz et al., 1999). This is in stark contrast to our observation of an appreciably larger angle of most probable tilt $\alpha_0 = 25°$ for $[3\alpha\text{-}^2H_1]$cholesterol in dipolyunsaturated 20:4–20:4PC bilayers. The implication is that the rigid sterol molecule prefers an environment of freely isomerizable saturated acyl chains, as opposed to polyunsaturated acyl chains containing multiple motionally constrained *cis* double bonds. Insensitivity of the orientation of cholesterol to polyunsaturation in heteroacid saturated-unsaturated PC bilayers reflects association with the saturated *sn*-1 chain to minimize contact with the polyunsaturated *sn*-2 chain, whereas in homoacid dipolyunsaturated 20:4–20:4PC bilayers, the sterol is forced to interact with polyunsaturated chains resulting in a greater angle of tilt and exclusion from the bilayer beyond ~15 mol% incorporation.

Cholesterol interaction with polyunsaturated versus saturated chains

Previously published studies offer additional evidence in support of preferential affinity of cholesterol for saturated over polyunsaturated chains. ^{1}H MAS NMR experiments on 18:0–22:6PC/$[25,26,26,26,27,27,27\text{-}^2H_7]$cholesterol (1:1 mol) membranes revealed closer contact with the 18:0 *sn*-1 chain via a higher rate of chain-to-cholesterol nuclear Overhauser enhancement spectroscopy cross-relaxation (Huster et al., 1998). A similar inference may be drawn from ^{2}H NMR data, indicating that the response of membrane-ordering and phase behavior to the introduction of cholesterol into mixed chain PC bilayers with a saturated *sn*-1 chain changes little in the presence of polyunsaturation at the *sn*-2 position. Essentially the same increase in orientational order was observed for the saturated $[^2H_{31}]$palmitoyl ($[^2H_{31}]$16:0) *sn*-1 chain in liquid crystalline $[^2H_{31}]$16:0–20:4PC as in 1-$[^2H_{31}]$ palmitoyl-2-linoleoylphosphatidylcholine ($[^2H_{31}]$16:0–18:2PC), $[^2H_{31}]$16:0–18:1PC, and $[^2H_{31}]$16:0–16:0PC (Vist and Davis, 1990; Thewalt and Bloom, 1992; Morrow at al., 1996; Jackman et al., 1999). The elevation is predominantly in the characteristic plateau region of approximately uniform order in the upper portion of the chain, whereas in the lower portion where order gradually decreases toward the disordered center of the membrane, the effect is diminished.

An attempt to definitively explain why cholesterol avoids proximity to PUFAs is premature on the basis of our current knowledge. Superficially, it may be speculated that saturated fatty acid offers a smooth façade favorable to close approach of the rigid steroid moiety, whereas PUFA presents a "rough" surface. The plateau region of almost constant order universally seen in the upper portion of saturated chains in liquid crystalline phospholipid bilayers is attributable to a preponderance of *trans* isomeric states aligning segments parallel to the bilayer normal (Schindler and Seelig, 1975; Douliez et al., 1995). A more irregular profile of molecular organization is anticipated for PUFA containing double bonds about which isomerization is prohibited.

Further speculation would entail an understanding of the conformation and dynamics of PUFA which remains controversial (Bloom et al., 1999). Narrow, multicomponent ^{2}H NMR spectra were observed for vinyl perdeuterated 16:0-[5,6,8,9,11,12,14,15-^{2}H$_8$]20:4PC and 16:0-[4,5,7,8,10,11,13,14,16,17,19,20-^{2}H$_{12}$]22:6PC membranes (Dratz and Deese, 1986; Rajamoorthi and Brown, 1991). A well defined structure in which the C-^{2}H bonds have an average orientation in the vicinity of the magic angle (54.7°) with respect to the bilayer normal is a possible interpretation. The rigidity of double bonds might be expected to restrict mobility. An alternative interpretation is a high degree of disorder. Molecular models for 1,4-pentadiene suggest that there is a reduced energy barrier to rotational isomerization about the single C-C bonds which separate the unsaturated carbons atoms in PUFA (Applegate and Glomset, 1986). Support for high conformational flexibility is provided by ^{13}C and ^{1}H MAS NMR work on 16:0–22:6PC membranes (Everts and Davis, 2000). Cross-peaks between the choline group and 22:6 chain in 2-D cross-polarization spectra demonstrated that the polyunsaturated chain approaches the membrane surface, and rotating frame-spin lattice relaxation measurements indicated that methylene groups in the 22:6 chain undergo motions with correlation times in the 10^{-6} s range. Rapid structural transitions including the adoption of looped conformations have also been described on the basis of order parameters measured with perdeuterated 22:6 acid and molecular dynamics simulations (Gawrisch et al., 2001). Another recent molecular dynamics study of 18:0–22:6PC bilayers also showed that the carbon atoms at the end of the chains and those participating in the double bonds can reach the lipid water interface (Saiz and Klein, 2001).

The consequences of incompatibility between sterol and PUFA will be particularly pronounced when cholesterol is introduced into a dipolyunsaturated phospholipid membrane and must be beside polyunsaturated chains. Two outcomes warranting discussion are that the sterol will be forced out of the membrane or will seek a region of saturated acyl chain within the hydrophobic interior. The "umbrella model" postulates that an increase in cholesterol/water contacts leads to the formation of cholesterol monohydrate which is then excluded from the membrane when the polar headgroups can no longer sufficiently shelter membrane-intercalated sterol from interfacial waters (Huang and Feigenson, 1999). Highly polyunsaturated bilayers are significantly more permeable to water than less unsaturated bilayers (Huster et al., 1997), enhancing the likelihood of near approach from water molecules and providing a plausible mechansim by which exclusion of cholesterol from 20:4–20:4PC membranes would be promoted via formation of monohydrate. An intriguing possibility is that sterol remaining within the 20:4–20:4PC membrane penetrates deeply into the hydrophobic core of the bilayer where it protrudes between monolayers to avoid the sequence of

methylene-interupted *cis* double bonds which runs from carbons C5 to C15 in 20:4 acid. The 5 single C-C bonds at the terminal methyl end of each 20:4 chain constitute a 10 carbon stretch between opposing leaflets with a maximum thickness in all-*trans* configuration of ~12.7 Å that could potentially accommodate the rigid ring system (~11 Å in length) of the cholesterol molecule. In support of interdigitation, quasielastic neutron scattering has indicated that cholesterol penetrates dynamically between leaflets of 16:0–16:0PC in the *lo*-phase (Gliss et al. 1999). Movement of cholesterol toward the hydrophobic core of fluid 14:0–14:0PC bilayers has also been discussed in a recent time-resolved small-angle x-ray study (Richter et al., 2001). We have neutron scattering experiments underway to identify the depth to which cholesterol locates in dipolyunsaturated 20:4–20:4PC and 22:6–22:6PC.

In light of the current work, it is possible to reconcile the relative lack of response to cholesterol seen for the thermodynamic and micromechanical properties of dipolyunsaturated systems as compared with their mixed saturated-polyunsaturated counterparts in terms of solubility to sterol. Time-resolved fluorescence of 1,6-diphenyl-1,3,5-hexatriene in a series of homoacid and heteroacid PCs showed that the presence of 30 mol% cholesterol appreciably restricts molecular motion in all bilayers except 20:4–20:4PC and 22:6–22:6PC (Mitchell and Litman, 1998). The impact is much less in the dipolyunsaturated membranes. Whereas ≥35 mol% sterol abolishes the gel to liquid crystalline phase transition in 16:0–20:4PC and 16:0–22:6PC (Hernandez-Borrell and Keough, 1993), up to 50 mol% cholesterol does little to the temperature or enthalpy of the transition in 20:4–20:4PC or 22:6–22:6PC (Kariel et al., 1991). The simple explanation that now may be ventured is that only a small amount of cholesterol intercalates into the dipolyunsaturated membranes. Poor mixing of cholesterol with 20:4–20:4 and 22:6–22:6PC is also implied by elastic compressibility moduli C_s^{-1} measured in monolayer films containing >30 mol% sterol (Smaby et al., 1997). The experimental C_s^{-1} values approximate the sum of the apportioned compressibility for each lipid, unlike with 16:0–20:4PC and 16:0–22:6PC, in which a reduction in native compressibility of the equivalent mixed chain phospholipids is indicated.

Mixed phospholipid membranes

Cholesterol-induced, lateral-phase separation

Differential affinity of cholesterol for polyunsaturated versus saturated acyl chains has been invoked as a lipid-driven mechanism for lateral-phase separation into PUFA-rich/cholesterol-poor and PUFA-poor/cholesterol-rich microdomains within cell membranes (Huster et al., 1998; Mitchell and Litman, 1998). The basic premise is that within mixed membranes, the sterol separates into patches minimizing

contact with polyunsaturated acyl chains. Segregation of lipids into compositionally distinct regions is thought to be essential for optimal protein function. For example, the activity of glycosyl-phosphatidylinositol-linked and acylated proteins relies upon their insertion into tightly packed cholesterol-rich regions (Simons and Ikonen, 1997). The ability of cholesterol and polyunsaturated lipids to modulate the functional activity of rhodopsin (Albert et al., 1996; Brown 1994; Polozova and Litman, 2000) and the nicotinic acetylcholine receptor (Rankin et al., 1997) serves to emphasize the possible importance of cholesterol/dipolyunsaturated PC-mediated domain formation in controlling local molecular organization. Favorable interaction with saturated chains, moreover, may be integral to the existence of highly saturated sphingolipid/cholesterol rafts (Brown and London, 2000). These membrane fragments and their potential role in cell signaling have been the subject of considerable attention recently. However, definitive confirmation that microdomains form within fluid membranes remains to be presented.

On the basis of the vastly disparate solubilities to cholesterol measured here, mixed membranes of 20:4–20:4PC and 18:0–20:4PC constitute a good candidate for the existence of domains. We chose to investigate a lipid mixture comprised of 20:4–20:4PC/18:0–20:4PC/[3α-^{2}H$_1$]cholesterol in a 1/1/2 mol ratio. This composition ensures that if sterol preferentially associates with equimolar heteroacid saturated-polyunsaturated phospholipid in patches, there is an excess of cholesterol remaining that must come into contact with dipolyunsaturated phospholipid. Fig. 2 illustrates that the ^{2}H NMR spectrum recorded (Fig. 2 C) qualitatively resembles that obtained with 20:4–20:4PC/[3α-^{2}H$_1$]cholesterol (1/1 mol) (Fig. 2 A). A narrow spectral component attributable to membrane-incorporated sterol is superposed upon a broad component because of solid sterol. Their relative intensities equate to solubility $\chi_{chol}^{NMR} = 40 \pm 2$ mol% in the mixed membrane which, as can be seen in Table 1, agrees within experimental uncertainty with the value $\chi_{chol}^{XRD} = 36 \pm 3$ mol% estimated from XRD. The same two spectral components are evident in the depaked ^{2}H NMR spectrum shown in Fig. 3 for 20:4–20:4PC/18:0–20:4PC/[3α-^{2}H$_1$]cholesterol (1/1/2 mol). A well resolved, inner doublet attributable to sterol incorporated into the membrane is flanked by an outer doublet attributable to solid sterol (Fig. 3 C). The observation that only a single signal arises from within the membrane is pivotal. It establishes that all [3α-^{2}H$_1$]cholesterol intercalated into the mixed membrane samples the same environment or environments on the 2×10^{-5}-s timescale of the ^{2}H NMR experiment (Bloom and Thewalt, 1995). The simplest interpretation has sterol uniformly distributed with tilt angle $\alpha_0 = 17°$ throughout a homogeneous 1/1 mol mixture of 20:4–20:4PC and 18:0–20:4PC. We consider this arrangement to be unlikely because the solubility of ~40 mol% measured would necessitate close proximity to

dipolyunsaturated phospholipid. Instead, we propose that motionally inequivalent 20:4–20:4PC/cholesterol-poor and 18:0–20:4PC/cholesterol-rich microdomains exist between which fast exchange mediated by lateral diffusion causes collapse of two distinct powder patterns to a population-weighted average signal.

Microdomain model

Support for our proposal is garnered when we compare the results for the mixed membrane with the predictions of an analysis in terms of the data on each constituent phospholipid membrane. In the model, 20:4–20:4PC and 18:0–20:4PC microdomains phase-separate containing the solubility limit of cholesterol determined for the two phospholipids individually (Table 1). Molecular organization of [3α-^{2}H$_1$]cholesterol in a microdomain is presumed to match that seen in 20:4–20:4PC or 18:0–20:4PC alone. The corresponding stoichiometry for the mixed 20:4–20:4PC/18:0–20:4PC/cholesterol$_{20:4-20:4PC}$/cholesterol$_{18:0-20:4PC}$/cholesterol$_{solid}$ system is 1.0/1.0/0.2/1.0/0.8 mol where the subscripts specify environment. A calculation via Eq. 6 demonstrates that this stoichiometry ($f_{int} = 1.2$ and $f_{PC} = 2.0$) represents a solubility of 38 mol% for cholesterol in 20:4–20:4PC/18:0–20:4PC (1/1 mol), which is comparable with the experimental value of ~40 mol%. Assuming the same stoichiometry and taking the quadrupolar splittings measured for [3α-^{2}H$_1$]cholesterol intercalated into 20:4–20:4PC and 18:0–20:4PC membranes (Table 1) to apply to the microdomains, it is then possible to predict the ^{2}H NMR spectrum for [3α-^{2}H$_1$]cholesterol incorporated into the mixed system according to our model. A superposition of two easily discernible powder patterns possessing quadrupolar splittings $\Delta\nu_r = 33$ kHz and $\Delta\nu_r = 45$ kHz, respectively, from 20:4–20:4PC and 18:0–20:4PC environments would be expected in the absence of exchange between microdomains. Their intensities would be in proportion to the relative concentration of [3α-^{2}H$_1$]cholesterol in the two environments. Inspection of powder pattern (Fig. 2 C) and depaked (Fig. 3 C) ^{2}H NMR spectra definitely shows only one spectral component characterizes [3α-^{2}H$_1$]cholesterol incorporated into 20:4–20:4PC/18:0–20:4PC (1/1 mol) membranes. A single spectral component would be produced, however, by the fast exchange of [3α-^{2}H$_1$]cholesterol between microdomains. The resultant quadrupolar splitting would be a population-weighted average given by

$$\Delta\nu_r = f^{20:4-20:4PC}\Delta\nu_r^{20:4-20:4PC} + f^{18:0-20:4PC}\Delta\nu_r^{18:0-20:4PC} \quad (7)$$

where $f^{20:4-20:4PC}$ and $f^{18:0-20:4PC}$ are the fractions of membrane incorporated [3α-^{2}H$_1$]cholesterol in a microdomain, $\Delta\nu_r^{20:4-20:4PC}$ and $\Delta\nu_r^{18:0-20:4PC}$ are the quadrupolar splittings associated with the microdomain and the superscripts specify 20:4–20:4PC and 18:0–20:4PC environments. Substitu-

20:4-20:4PC/cholesterol
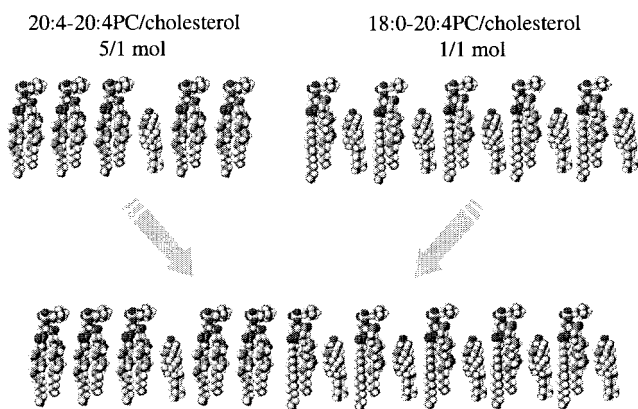5/1 mol

18:0-20:4PC/cholesterol
1/1 mol

FIGURE 6 Schematic depiction that homoacid dipolyunsaturated phospholipid/cholesterol-poor and heteroacid saturated-polyunsaturated phospholipid/cholesterol-rich microdomains form in mixed membranes. Solubility and molecular orientation of sterol in a microdomain closely resemble within a separate membrane composed of the appropriate phospholipid.

tion into this expression using the values from our model ($f^{20:4-20:4PC} = 0.17$ and $f^{18:0-20:4PC} = 0.83$, and $\Delta\nu_r^{20:4-20:4PC} = 33$ kHz and $\Delta\nu_r^{18:0-20:4PC} = 45$ kHz) yields $\Delta\nu_r = 43$ kHz. Within experimental error, the calculated splitting agrees with the experimentally observed splitting of $\Delta\nu_r = 44 \pm 1$ kHz for $[3\alpha\text{-}^2H_1]$cholesterol incorporated into 20:4–20:4PC/18:0–20:4PC (1/1 mol) membranes (Table 1).

The data obtained on the mixed 20:4–20:4PC/18:0–20:4PC (1:1 mol) system are thus consistent with phase separation into 20:4–20:4PC/cholesterol and 18:0–20:4PC/cholesterol microdomains preserving the solubility and molecular organization seen for the sterol in membranes of the individual phospholipids. It should be noted, nonetheless, that the interpretation is not unique. Neither a single-site model nor fast exchange between multiple sites can be ruled out. A schematic representation of our two-site model is depicted in Fig. 6. The general features resemble a model presented by Mitchell and Litman (1998), who envisaged transient, highly dynamic microdomains in which cholesterol is surrounded by heteroacid saturated-polyunsaturated PC molecules with their saturated sn-1 chain pointed toward the interior of the domain and the polyunsaturated sn-2 chain oriented toward the domain boundary. Dipolyunsaturated PC molecules provide the phase-connecting microdomains. The fast exchange prescribed by our analysis implies that the lifetime of $[3\alpha\text{-}^2H_1]$cholesterol in a microdomain must be less than $\tau = (2\pi\Delta\nu)^{-1} = 1.3 \times 10^{-5}$ s, where $\Delta\nu = 12$ kHz is the difference between quadrupolar splittings in the microdomains taken from the ^{2}H NMR spectra for $[3\alpha\text{-}^2H_1]$cholesterol in 20:4–20:4PC and 18:0–20:4PC independently (Figs. 2, A and B). Lateral diffusion described by $D \sim 5 \times 10^{-12}$ m^2/s (Lindblom and Oradd, 1994) within the plane of the membrane is the mechanism of exchange, and an upper limit of <160 Å is placed upon microdomain radius in the 20:4–20:4PC/18:0–20:4PC/$[3\alpha\text{-}^2H_1]$cholesterol (1/1/2 mol) system by estimating the concomitant root mean square displacement $r = (4D\tau)^{1/2}$ from the lifetime. Such microdomains, if treated as circular, would contain <1300 lipid molecules of mean cross-sectional area 60 Å^2 in each leaflet. Segregation of rhodospin with dipolyunsaturated phospholipid into clusters with radius 35 Å, equivalent to two annular layers of lipid around the protein, was recently concluded from fluorescence resonance energy transfer measurements on proteoliposomes containing 22:6–22:6PC, 16:0–16:0PC, and cholesterol (Polozova and Litman, 2000). The upper limit to microdomain size evaluated here could certainly accommodate these clusters, although the apparent compatibility may be misleading as an inability to detect clustering in protein-free bilayers was also noted.

CONCLUSION

Low affinity of cholesterol to phospholipid-containing PUFA was conclusively demonstrated by a complementary combination of ^{2}H NMR and XRD experimental approaches in this study. When cholesterol was added to dipolyunsaturated 20:4–20:4PC, only ~15 mol% could be incorporated into the membrane whereas any excess was excluded as monohydrate crystals. This solubility represents an enormous reduction over the ~50 mol% concentration of cholesterol that can reside within saturated-polyunsaturated 18:0–20:4PC membranes. Further indication of substantial differential in interaction with PUFA versus saturated fatty acid was provided by evaluation of a much greater tilt angle for the steroid moiety in 20:4–20:4PC ($\alpha_0 = 25°$) than in 18:0–20:4PC ($\alpha_0 = 16°$). A model that successfully reproduces data on mixed 20:4–20:4PC/18:0–20:4PC (1/1 mol) membranes was presented in which cholesterol induces phase separation into dipolyunsaturated PC/cholesterol-poor and saturated-polyunsaturated PC/cholesterol-rich microdomains matching the molecular organization of sterol in each phospholipid. A maximum limit of <160 Å applies to the size of the microdomains. The model is compatible with the existence of localized PUFA-rich/cholesterol-poor regions that are hypothesized to be essential for the functioning of certain neuronal proteins.

REFERENCES

Albert, A. D., K. Booesze-Battaglia, Z. Paw, A. Watts, and R. M. Epand. 1996. Effect of cholesterol on rhodopsin stability in disk membranes. *Biochim. Biophys. Acta.* 1297:77–82.

Applegate, K. R., and J. A. Glomset. 1986. Computer-based modeling of the conformation and packing properties of docosahexaenoic acid. *J. Lipid Res.* 27:658–680.

Aveldano, M. I. 1989. Dipolyunsaturated species of retina phospholipids and their fatty acids. *Colloq. INSERM.* 195:87–96.

Blanton, T. N., T. C. Huang, H. Toraya, C. R. Hubbard, S. B. Robie, D. Louer, H. E. Gobel, G. Will, R. Gilles, and T. Raftery. 1995. JCPDS–International Centre for Diffraction Data round robin study of silver behenate. A possible low-angle X-ray diffraction calibration standard. *Powder Diffraction.* 10:91–95.

Bloom, M., J. H. Davis, and M. I. Valic. 1980. Spectral distortion effects due to finite pulse widths in deuterium nuclear magnetic resonance spectroscopy. *Can. J. Phys.* 58:1510–1517.

Bloom, M., F. Linseisen, and J. Lloyd-Smith. 1999. Insights from NMR on the functional role of polyunsaturated lipids in the brain. *In* Proceedings of the International School of Physics 'Enrico Fermi', Course CXXXIX on: Magnetic Resonance and Brain Function: Approaches from Physics. B. Maraviglia, editor. IOS Press, Ohmsha, Germany. 527–553.

Bloom, M., and J. L. Thewalt. 1995. Time and distance scales of membrane domain organization. *Mol. Membrane Biol.* 12:9–13.

Bonmatin, J. M., I. C. Smith, H. C. Jarrell, and D. J. Siminovitch. 1990. Use of a comprehensive approach to molecular dynamics in ordered lipid systems: cholesterol reorientation in oriented lipid bilayers. *J. Amer. Chem. Soc.* 112:1697–1704.

Brown, D., and E. London. 2000. Structure and function of sphingo- and cholesterol-rich membrane rafts. *J. Biol. Chem.* 275:17221–17224.

Brown, M. F. 1994. Modulation of rhodopsin function by properties of the membrane bilayer. *Chem. Phys. Lipids* 73:159–180.

Brzustowicz, M. R., W. Stillwell, and S. R. Wassall. 1999. Molecular organization of cholesterol in polyunsaturated phospholipid membranes: a solid state ^{2}H NMR investigation. *FEBS Lett.* 451:197–202.

Brzustowicz, M. R., M. Zerouga, V. Cherezov, M. Caffrey, W. Stillwell, and S. R. Wassall. 2000. Solid state NMR and x-ray diffraction studies of cholesterol molecular organization in polyunsaturated phospholipid bilayers. *Biophys. J.* 78:184A.

Craven, B. M. 1976. Crystal structure of cholesterol monohydrate. *Nature.* 260:727–729.

Davis, J. H., K. R. Jeffrey, M. Bloom, M. I. Valic, and T. P. Higgs. 1976. Quadrupolar echo deuteron magnetic resonance spectroscopy in ordered hydrocarbon chains. *Chem. Phys. Lett.* 42:390–394.

Douliez, J. P., A. Leonard, and E. J. Dufourc. 1995. Restatement of order parameters in biomembranes: calculation of C-C bond order parameters from C-D quadrupolar splittings. *Biophys. J.* 68:1727–1739.

Dratz, E. A., and A. J. Deese. 1986. The role of docosahexaenoic acid (22:6ω3) in biological membranes: examples from photoreceptors and model membrane bilayers. *In* Health Effects of Polyunsaturated Fatty Acids in Seafoods. A. P. Simopoulos, R. R. Kifer, and R. E. Martin, editors. Academic Press, New York. 319–351.

Everts, S., and J. H. Davis. 2000. ^{1}H and ^{13}C NMR of multilamellar dispersions of polyunsaturated (22:6) phospholipids. *Biophys. J.* 79:885–897.

Finegold, L., editor. 1993. Cholesterol in Membrane Models. CRC Press, Boca Raton.

Gawrisch, K., S. E. Feller, N. V. Eldho, and A. M. Safley. 2001. Conformation and flexibility of the polyunsaturated docosahexaenoic acid chain. *Biophys. J.* 80:520a.

Gennis, R. B. 1989. Biomembranes. Springer-Verlag, New York.

Gliss, C., O. Randel, H. Casalta, E. Sackmann, R. Zorn, and T. Bayerl. 1999. Anisotropic motion of cholesterol in oriented DPPC bilayers studied by quasielastic neutron scattering: the liquid-ordered phase. *Biophys. J.* 77:331–340.

Guo, W., and J. A. Hamilton. 1995. A multinuclear solid-state NMR study of phospholipid-cholesterol interactions. Dipalmitoylphosphatidylcholine-cholesterol binary system. *Biochemistry.* 34:14174–14184.

Hammersley, A. P. 1997. FIT2D: An Introduction and Overview. ESRF Internal Report. Publication no. ESRF97HA02T. Grenoble, France.

Hernandez-Borrell, J., and K. M. Keough. 1993. Heteroacid phosphatidylcholines with different amounts of unsaturation respond differently to cholesterol. Biochim. Biophys. Acta.1153:277–282.

Huang, J., J. T. Buboltz, and G. W. Feigenson. 1999. Maximum solubility of cholesterol in phosphatidylcholine and phosphatidylethanolamine bilayers. *Biochim. Biophys. Acta.* 1417:89–100.

Huang, J., and G. W. Feigenson. 1999. A microscopic interaction model of maximum solubility of cholesterol in lipid bilayers. *Biophys. J.* 76:2142–2157.

Huang, T. H., C. W. Lee, S. K. Das Gupta, A. Blume, and R. G. Griffin. 1993. A ^{13}C and ^{2}H nuclear magnetic resonance study of phosphatidylcholine/cholesterol interactions: characterization of liquid-gel phases. *Biochemistry.* 32:13277–13287.

Huster, D., K. Arnold, and K. Gawrisch. 1998. Influence of docosahexaenoic acid and cholesterol on lateral lipid organization in phospholipid mixtures. *Biochemistry.* 49:17299–17308.

Huster, D., A. J. Jin, K. Arnold, and K. Gawrisch. 1997. Water permeability of polyunsaturated lipid membranes measured by ^{17}O NMR. *Biophys. J.* 73:855–864.

Jackman, C. S., P. J. Davis, M. R. Morrow, and K. M. Keough. 1999. Effect of cholesterol on the chain-ordering transition of 1-palmitoyl-2-arachidonoyl phosphatidylcholine. *J. Phys. Chem. B.* 103:8830–8836.

Jacob, R. F., R. J. Cenedella, and R. P. Mason. 1999. Direct evidence for immiscible cholesterol domains in human ocular lens fiber cell plasma membranes. *J. Biol. Chem.* 274:31613–31618.

Kariel, N., E. Davidson, and K. M. Keough. 1991. Cholesterol does not remove the gel-liquid crystalline transition of phosphatidylcholines containing two polyenoic chains. *Biochim. Biophys. Acta.* 1062:70–76.

Lindblom, G., and G. Oradd. 1994. NMR studies of translational diffusion in lyotropic liquid crystals and membranes. *Prog. NMR Spectroscopy.* 26:483–515.

Loomis, C. R., G. G. Shipley, and D. M. Small. 1979. The phase behavior of hydrated cholesterol. *J. Lipid Res.* 20:525–535.

Marsan, M. P., I. Muller, C. Ramos, F. Rodriguez, E. J. Dufourc, J. Czaplicki, and A. Milon. 1999. Cholesterol orientation and dynamics in dimyristoylphosphatidylcholine bilayers: a solid state deuterium NMR analysis. *Biophys. J.* 76:351–359.

McCabe, M. A., and S. R. Wassall. 1997. Rapid deconvolution of NMR powder spectra by weighted fast Fourier transformation. *Solid State Nucl. Mag. Reson.* 10:53–61.

McMullen, T. P., and R. N. McElhaney. 1996. Physical studies of cholesterol-phospholipid interactions. *Curr. Opin. Colloid Interface Sci.* 1:83–90.

Mitchell, D. C., and B. J. Litman. 1998. Effect of cholesterol on molecular order and dynamics in highly polyunsaturated phospholipid bilayers. *Biophys. J.* 75:896–908.

Monck, M. A., M. Bloom, M. Lafleur, R. N. Lewis, R. N. McElhaney, and P. R. Cullis. 1993. Evidence for two pools of cholesterol in the *Acholeplasma laidlawii* strain B membrane: a deuterium NMR and DSC study. *Biochemistry.* 32:3081–3088.

Morrow, M. R., P. J. Davis, C. S. Jackman, and K. M. Keough. 1996. Thermal history alters cholesterol effect on transition of 1-palmitoyl-2-linoleoyl phosphatidylcholine. *Biophys. J.* 71:3207–3214.

Murari, R., M. P. Murari, and W. J. Baumann. 1986. Sterol orientations in phosphatidylcholine liposomes as determined by deuterium NMR. *Biochemistry.* 25:1062–1067.

Oldfield, E., M. Meadows, D. Rice, and R. Jacobs. 1978. Spectroscopic studies of specifically deuterium labeled membrane systems. Nuclear magnetic resonance investigation of the effects of cholesterol in model systems. *Biochemistry.* 17:2727–2740.

Petersen, N. O., and S. I. Chan. 1977. More on the motional state of lipid bilayer membranes: interpretation of order parameters obtained from nuclear magnetic resonance experiments. *Biochemistry.* 16:2657–2667.

Phillips, M. C. 1990. Cholesterol packing, crystallization and exchange properties in phosphatidylcholine vesicle systems. *Hepatology.* 12: 75S–82S.

Polozova, A., and B. J. Litman. 2000. Cholesterol dependent recruitment of di22:6-PC by a G protein-coupled receptor into lateral domains. *Biophys. J.* 79:2632–2643.

Rajamoorthi, K., and M. F. Brown. 1991. Bilayers of arachidonic acid containing phospholipids studied by ^{2}H and ^{31}P NMR spectroscopy. *Biochemistry.* 30:4204–4212.

Rankin, S. E., G. H. Addona, M. A. Kloczewiak, B. Bugge, and K. W. Miller. 1997. The cholesterol dependence of activation and fast desensitization of the nicotinic acetylcholine receptor. *Biophys. J.* 73: 2446–2455.

Richter, F., G. Rapp, and L. Finegold. 2001. Miscibility gap in fluid dimyristoylphosphatidylcholine:cholesterol as "seen" by x rays. *Phys. Rev. E. Stat. Phys. Plasma Fluids Relat. Interdiscip. Topics.* 63:051914.

Rietveld, A., and K. Simons. 1998. The differential miscibility of lipids as the basis for the formation of functional membrane rafts. *Biochim. Biophys. Acta.* 1376:467–479.

Ruocco, M. J., D. J. Siminovitch, J. R. Long, S. K. Das Gupta, and R. G. Griffin. 1996. ^{2}H and ^{13}C nuclear magnetic resonance study of *N*-palmitoylgalactosylsphingosine (cerebroside)/cholesterol bilayers. *Biophys. J.* 71:1776–1788.

Saiz, L., and M. L. Klein. 2001. Structural properties of a highly polyunsaturated lipid bilayer from molecular dynamics simulations. *Biophys. J.* 81:204–216.

Salem, Jr., N., H. Y. Kim, and J. A. Yergey. 1986. Docosahexaenoic acid: membrane function and metabolism. *In* Health Effects of Polyunsaturated Fatty Acids in Seafoods. A. P. Simopoulos, R. R. Kifer, and R. E. Martin, editors. Academic Press, New York. 263–317.

Schindler, H., and J. Seelig. 1975. Deuterium order parameters in relation to thermodynamic properties of a phospholipid bilayer. A statistical mechanical interpretation. *Biochemistry.* 14:2283–2287.

Seelig, J. 1978. ^{31}P nuclear magnetic resonance and the head group structure of phospholipids in membranes. *Biochim. Biophys. Acta.* 515: 105–140.

Shieh, H. S., L. G. Hoard, and C. E. Nordman. 1977. Crystal structure of anhydrous cholesterol. *Nature.* 267:287–289.

Simons, K., and E. Ikonen. 1997. Functional rafts in cell membranes. *Nature.* 387:569–572.

Smaby, J. M., M. M. Momsen, H. L. Brockman, and R. E. Brown. 1997. Phosphatidylcholine acyl unsaturation modulates the decrease in interfacial elasticity induced by cholesterol. *Biophys. J.* 73:1492–1505.

Sömjen, G. J., G. Lipka, G. Schulthess, M. H. Koch, E. Wachtel, T. Gilat, and H. Hauser. 1995. Behavior of cholesterol and spin-labeled cholestane in model bile systems studied by electron spin resonance and synchrotron x-ray. *Biophys. J.* 68:2342–2349.

Sternin, E., M. Bloom, and A. L. MacKay. 1983. De-Pake-ing of NMR spectra. *J. Magn. Reson.* 55:274–282.

Taylor, M. G., T. Akiyama, H. Saito, and I. C. Smith. 1982. Direct observation of cholesterol in membranes by deuterium NMR. *Chem. Phys. Lipids.* 31:359–379.

Taylor, M. G., T. Akiyama, and I. C. Smith. 1981. The molecular dynamics of cholesterol in bilayer membranes: a deuterium NMR study. *Chem. Phys. Lipids.* 29:327–339.

Thewalt, J. L., and M. Bloom. 1992. Phosphatidylcholine: cholesterol phase diagrams. *Biophys. J.* 63:1176–1181.

Vist, M. R., and J. H. Davis. 1990. Phase equilibria of cholesterol/dipalmitoylphosphatidylcholine mixtures: ^{2}H nuclear magnetic resonance and differential scanning calorimetry. *Biochemistry.* 29:451–464.

Zhang, Q. W., H. Zhang, K. V. Lakshmi, D. K. Lee, C. H. Bradley, and R. J. Wittebort. 1998. Double and triple resonance circuits for high-frequency probes. *J. Magn. Reson.* 132:167–171.

Zhu, T., and M. Caffrey. 1993. Thermodynamic, thermomechanical and structural properties of a hydrated asymmetric phosphatidylcholine. *Biophys. J.* 65:939–954.